Electric Power Systems Research 131 (2016) 87–95

Contents lists available at ScienceDirect

Electric Power Systems Research

journal homepage: www.elsevier.com/locate/epsr

Coordinated excitation and steam valve control for multimachine power system using high order sliding mode technique

Godpromesse Kenné*, Andrew Muluh Fombu, Jean de Dieu Nguimfack-Ndongmo

Laboratoire d'Automatique et d'Informatique Appliquée (LAIA), Département de Génie Electrique, IUT FOTSO Victor Bandjoun, Université de Dschang, B.P. 134 Bandjoun, Cameroon

ARTICLE INFO

Article history:
Received 4 February 2015
Received in revised form 11 July 2015
Accepted 2 October 2015

Keywords:
Multi-machine power system
High order sliding mode control
Excitation control
Steam-valve control
Adaptive control

ABSTRACT

This paper presents a decentralized coordinated excitation and steam valve adaptive control combined with a high-order sliding mode differentiator. The aim is to obtain high performance for the terminal voltage and the rotor speed simultaneously under a sudden fault and a wide range of operating conditions. The methodology adopted is based on second order sliding mode technique using the supper twisting algorithm. The proposed scheme requires only local information on the physically available measurements of relative angular speed, active electric power and terminal voltage with the assumption that the power angle and mechanical power input are not available for measurement. It can be implemented locally and dispersedly for individual generators and is convenient for industrial applications. Simulation results in the case of the Kundur 4-machines 2-area power system show the effectiveness, robustness and superiority of the proposed scheme over the classical AVR/PSS controller and steam valve PI regulator.

1. Introduction

Power systems are becoming increasingly more complex due to the interconnection of regional subsystems, deregulations and the operation of associated electricity markets. As a result, they require the application of advanced control techniques to improve their dynamic performance and stability. Since the generator subsystems are interconnected in wide geographical areas, decentralized control is preferred because it does not require the full state feedback and communication between different subsystems, which makes the controller implementation more feasible and simpler [1–3].

Recently, to cope with the increasing demand for quality electric power, much attention has been given to the application of nonlinear control techniques to solve the transient stability problem. Nonlinear control techniques such as feedback linearization [4,5], Hamiltonian techniques [6], passivity base approach [7], singular perturbation [8], and sliding mode control [9–12] have been successfully applied to achieve high dynamic performance under large sudden faults.

Amongst these nonlinear techniques, sliding mode control has been recognized as one of the efficient tools to design robust controllers for complex high order nonlinear dynamic systems operating under various uncertainty conditions. The main advantage of sliding mode is the low sensitivity to plant parameter variations and disturbances which relaxes the necessity of exact modeling [13]. Despite this advantage, the usage of standard sliding mode is restricted due to the chattering effect caused by the control switching. High order sliding mode (HOSM) technique generalizes the basic sliding mode idea by acting on the higher order time-derivative of the sliding manifold, instead of influencing the first time-derivative as it is the case in the standard sliding mode [14]. The operational feature of HOSM allows mitigating the chattering effect while keeping the main properties of the original approach.

Nonlinear control using the excitation of synchronous generators [4,11,15,16] is a viable option to improve the stability margin when economic constraints do not permit the use of FACTS equipments. In this way, a cheaper solution based on the existing power system facilities is obtained. Nevertheless, the improvement of transient stability is limited due to the physical limits of the excitation voltage. In order to further improve the transient stability, it has been shown in [4,17–19] that a decentralized control should also be applied to the valve opening of steam turbines or hydroturbines. The problem of frequency control is also very important in all power systems. The system is in equilibrium when the generated power is equal to the consumed power. This equilibrium is maintained by the control of the power generated by the prime movers (steam turbines) [20].

* Corresponding author. Tel.: +237 677 59 52 19.
E-mail addresses: gokenne@yahoo.com, godpromesse.kenne@univ-dschang.org (G. Kenné), fombuandrewmuluh@yahoo.com (A.M. Fombu), nguimfackjdedieu@yahoo.fr (J.d.D. Nguimfack-Ndongmo).

http://dx.doi.org/10.1016/j.epsr.2015.10.003
0378-7796/

More recently, various advanced nonlinear control technologies have been applied to excitation and steam valve control design of single machine and multi-machine power systems [2,11,15,18,19]. However, in most cases, the turbine and excitation controls are considered as independent and decoupled processes characterized by different time scales, which is unsuitable for modern power systems since the appearance of advanced governors, such as digital governors, results in tight mutual interaction between excitation and governor loops [17,18]. Furthermore, most of these nonlinear control schemes are based on the Direct Feedback Linearization (DFL) technique and differential geometric tools which reduces or cancels the inherent system nonlinearities in order to obtain a feedback equivalent linear system.

Some recent results can be found in [2,11,15,18,19,6,21]. In [2], a nonlinear decentralized scheme was developed to solve the problem of general nonlinear bounds of interconnections. Both excitation and steam valve control were developed to enhance the transient stability. Nevertheless, DFL is used and the problem of voltage regulation has not been addressed. In [11], a sliding mode controller based on a time-varying sliding surface is used to control the rotor speed and terminal voltage simultaneously in order to enhance the transient stability and to ensure good post-fault voltage regulation. But in practice, the selection of a time-varying sliding surface is a difficult task. Also, the case of a multi-machine power system has not been investigated. In [15], a multi-variable nonlinear controller is proposed to achieve simultaneously rotor angle stability and good quality post-fault regulation of the generator terminal voltage, taking into account the automatic voltage and speed regulators dynamics in the control design. However, the problem is formulated as a tracking problem based on differential geometric tools which linearizes the system.

A nonlinear decentralized excitation and governor coordinated controller design for hydraulic power plants is proposed in [18] to enhance power system transient stability. But the excitation and hydro-governor controllers, are developed based on differential geometric theory and the problem of voltage regulation has not been investigated. It has been shown in [19] that a robust coordinated excitation and steam valve control produce better results when a large fault occurs close to the generator terminal. However, DFL is used and the coordination between the two control laws is done using a switching algorithm which causes a discontinuity of system behavior. Hence the control laws cannot achieve satisfactorily both transient stability enhancement and voltage regulation simultaneously. In [6], the stabilization of generalized Hamiltonian control system with internally generated energy is considered using passivity-based control. Both steam valve control and super-conducting magnetic energy storage (SMES) control were developed to enhance the transient stability. However, the problem of voltage regulation has not been investigated.

In order to satisfy some recent objectives and constraints imposed by the evolution of large scale interconnected power systems, a new methodology for the synthesis of power system stabilizers (PSSs) and speed governors using a third level of coordination is proposed in [21]. Both Standard PSSs and improved governors were developed and tuned simultaneously in a coordinated way in order to achieve the desired performance. However, the control model is obtained by linearizing the nonlinear power system around a given operation point. In addition, most of the above control algorithms assumes that the mechanical power input and power angle are available. But these parameters or variables are physically not available for measurement in practice.

Due to the above mentioned issues and by exploiting the concepts developed in [16,22], in this paper we propose:

- A simplified nonlinear decentralized coordinated excitation and steam valve adaptive control based on the supper twisting algorithm to simultaneously enhance the transient stability and voltage regulation of a multi-machine power system with unknown power angle and mechanical power input.
- A high-order sliding mode differentiator to estimate the time derivatives of unmeasurable variables and states.
- Numerical simulations to test the interaction and compare the performance of the new nonlinear adaptive control scheme with the classical AVR/PSS controller and steam valve PI regulator.

The paper is organized as follows. In Section 2, the dynamic model of the multi-machine power system is described. The design procedure of the formulation of the proposed control algorithms is presented in Section 3. Simulation results are presented in Section 4 to demonstrate the performance of the proposed controllers. Finally, in Section 5, some concluding remarks end the paper.

2. Plant system dynamic model and control objectives

2.1. Multi-machine dynamic model

The full mathematical details and physical assumptions of the classical dynamic model of a large scale power systems can be found in [23–25,17]. In this work, we use the following dynamics and electrical equations.

Mechanical dynamics:

$$\dot{\delta}_i = \omega_i, \tag{1}$$

$$\dot{\omega}_i = -\frac{D_i}{H_i}\omega_i - \frac{\omega_s}{H_i}(P_{ei} - P_{mi}). \tag{2}$$

Generator electrical dynamics:

$$\dot{E}'_{qi} = \frac{1}{T'_{doi}}(E_{fi} - E_{qi}). \tag{3}$$

Turbine dynamics:

$$\dot{P}_{mi} = -\frac{1}{T_{mi}}P_{mi} + \frac{K_{mi}}{T_{mi}}X_{ei}. \tag{4}$$

Turbine valve control:

$$\dot{X}_{ei} = -\frac{K_{ei}}{T_{ei}R_i\omega_s}\omega_i - \frac{1}{T_{ei}}X_{ei} + \frac{1}{T_{ei}}P_{ci}. \tag{5}$$

Electrical equations:

$$E_{qi} = x_{adi}I_{fi} = E'_{qi} + (x_{di} - x'_{di})I_{di}, \tag{6}$$

$$E_{fi} = K_{ci}u_{fi}, \tag{7}$$

$$P_{ei} = \sum_{j=1}^{n} E'_{qi}E'_{qj}B_{ij}\sin(\delta_i - \delta_j), \tag{8}$$

$$Q_{ei} = -\sum_{j=1}^{n} E'_{qi}E'_{qj}B_{ij}\cos(\delta_i - \delta_j), \tag{9}$$

$$I_{di} = -\sum_{j=1}^{n} E'_{qj}B_{ij}\cos(\delta_i - \delta_j), \tag{10}$$

$$I_{qi} = \sum_{j=1}^{n} E'_{qj}B_{ij}\sin(\delta_i - \delta_j), \tag{11}$$

$$V_{ti} = \sqrt{(E'_{qi} - x'_{di}I_{di})^2 + (x'_{di}I_{qi})^2}. \tag{12}$$

The notation for the multimachine power system model is given in Appendix A.1.

2.2. Control objectives

We design independently two controllers based on local measurements for each machine, i.e., E_{fi} for the excitation control loop and P_{ci} for the steam valve control loop and coordinate their actions in order to cooperatively achieve both transient stability enhancement and voltage regulation simultaneously in the presence of a large perturbation. The interactions between machines are considered as perturbations and are compensated by the robust controller.

3. Adaptive controller design

In this section we apply the second order sliding mode control (SOSMC) technique using the supper twisting algorithm for multi-machine power system control. The algorithm has been developed for the case where the relative degree of the system is 1 in order to mitigate the chattering phenomenon. For this purpose, the following assumption will be considered until further notice:

Assumption (i). It is assumed that the outputs/states of the system are continuous and bounded.

Since E'_{qi} is not measurable in practice, it is convenient to express the generator electrical dynamics in terms of the active electrical power.

The simplified expressions of active power P_{ei} and reactive power Q_{ei} are given by:

$$P_{ei} = E'_{qi} I_{qi} = \frac{E'_{qi} V_{ti} \sin(\delta_i - \theta_i)}{x'_{di}} \tag{13}$$

$$Q_{ei} = -E'_{qi} I_{di} = \frac{V_{ti}^2}{x'_{di}} - \frac{E'_{qi} V_{ti} \cos(\delta_i - \theta_i)}{x'_{di}} \tag{14}$$

where θ_i is the terminal voltage reference angle in radians. The dq components of the terminal voltage are given by:

$$V_{tid} = V_{ti} \sin(\delta_i - \theta_i) = x'_{di} I_{qi} \tag{15}$$

$$V_{tiq} = V_{ti} \cos(\delta_i - \theta_i) = E'_{qi} - x'_{di} I_{di} \tag{16}$$

The time derivative of (13) can be obtained using (3) and (6) as:

$$\dot{P}_{ei} = -\frac{1}{T'_{doi}} P_{ei} + \frac{1}{T'_{doi}} \left[(E_{fi} - (x_{di} - x'_{di}) I_{di}) I_{qi} + T'_{doi} \frac{P_{ei} \dot{I}_{qi}}{I_{qi}} \right]. \tag{17}$$

Remark 1. In the model described by (1)–(12) the power angle δ_i and the mechanical power input P_{mi} are assumed not to be available for measurement.

To this end, the results of the finite time convergence estimation algorithm of the mechanical power proposed in [16,5] will be applied in this paper. The power angle estimation δ_i is computed online using the expression derived from (13)–(16) as follows:

$$\delta_i = \operatorname{arccot}\left(\frac{V_{ti}}{x'_{di} P_{ei}} \sqrt{A_i^2 - B_i^2} \right) + \theta_i \tag{18}$$

with $A_i = \sqrt{V_{ti}^2 - (x'_{di} I_{qi})^2} + x'_{di} I_{di}$ and $B_i = \frac{P_{ei} x'_{di}}{V_{ti}}$.

3.1. High order sliding mode excitation controller

In order to derive the control law, we recall and rewrite the state space model using (1), (2) and (17) as follows:

$$\begin{aligned} \dot{\delta}_i &= \omega_i, \\ \dot{\omega}_i &= -\frac{D_i}{H_i}\omega_i - \frac{\omega_s}{H_i}(P_{ei} - P_{mi}), \\ \dot{P}_{ei} &= -\frac{1}{T'_{doi}} P_{ei} + \frac{1}{T'_{doi}} V_{fi}, \end{aligned} \tag{19}$$

$$\text{where} \quad V_{fi} = (E_{fi} - (x_{di} - x'_{di}) I_{di}) I_{qi} + T'_{doi} \frac{P_{ei} \dot{I}_{qi}}{I_{qi}} \tag{20}$$

has been used to simplify the notation.

Consider the following coordinate transformation:

$$\eta_i = \delta_i - \delta_{iref} + \beta_{0i}\omega_i = \tilde{\delta}_i + \beta_{0i}\omega_i \tag{21}$$

where $\beta_{0i} > 0$ is a design parameter and $\tilde{\delta}_i = \delta_i - \delta_{iref}$ is the power angle tracking error. The reference trajectory δ_{iref} can be obtained from (18) as:

$$\delta_{iref} = \operatorname{arccot}\left(\frac{V_{tiref}}{x'_{di} P_{mi}} \sqrt{A_{iref}^2 - B_{iref}^2} \right) + \theta_i \tag{22}$$

with $A_{iref} = \sqrt{V_{tiref}^2 - (x'_{di} I_{qi})^2} + x'_{di} I_{di}$ and $B_{iref} = \frac{P_{mi} x'_{di}}{V_{tiref}}$.

To ensure the boundedness of the trajectory in the new coordinate η_i and also that

$$\lim_{t \to +\infty} \eta_i(t) = 0,$$

we take

$$T_i = \eta_i + a_{1i} \int \eta_i dt \tag{23}$$

and, we calculate the reference signal P^*_{ei} which is the unique solution of $\dot{T}_i = 0$ as follows:

$$P^*_{ei} = \frac{H_i}{\beta_{oi}\omega_s} \left[a_{1i}\eta_i + \omega_i \left(1 - \beta_{oi}\frac{D_i}{H_i} \right) \right] + P_{mi}. \tag{24}$$

Next, we find the control input E_{fi} such that the closed-loop system is exponentially stable at the operating point. To this end, consider the following switching surface

$$\sigma_{1i} = P_{ei} - P^*_{ei}, \tag{25}$$

whose second time derivative is:

$$\ddot{\sigma}_{1i} = \ddot{P}_{ei} - \ddot{P}^*_{ei}. \tag{26}$$

Substituting $\ddot{P}_{ei}$ obtained using (19) into (26), yields:

$$\ddot{\sigma}_{1i} = \frac{1}{T'_{doi}} \dot{V}_{fi} - \frac{1}{T'_{doi}} \dot{P}_{ei} - \ddot{P}^*_{ei} \tag{27}$$

which can be simplified into:

$$\ddot{\sigma}_{1i} = \frac{1}{T'_{doi}} u_{1i} + G_{1i} \tag{28}$$

where $u_{1i} = \dot{V}_{fi}$ is an auxiliary control variable to be designed in order to satisfy the control objective of steering σ_{1i} and its derivative to zero and $G_{1i} = -\left(\frac{1}{T'_{doi}} \dot{P}_{ei} + \ddot{P}^*_{ei} \right)$ is an uncertain term.

In order to derive the super-twisting algorithm, the following assumption is required [26]

Assumption (ii). There exists positive constants S_{0i}, K_{m1i}, K_{M1i}, Φ_{1i}, such that $\forall P_{ei} \in \Re$ and $|S(P_{ei}, t)| > S_{0i}$, the following inequality holds:

$$|G_{1i}| \leq \Phi_{1i} \quad \text{and} \quad 0 < K_{m1i} \leq \frac{1}{T'_{doi}} \leq K_{M1i}. \tag{29}$$

Under the above conditions, if the control gains are chosen as:

$$\alpha_{1i} > \frac{\Phi_{1i}}{K_{m1i}} \quad \text{and} \quad \beta_{1i}^2 \leq \frac{4\Phi_{1i}}{K_{m1i}^2}\frac{K_{M1i}(\alpha_{1i}+\Phi_{1i})}{K_{m1i}(\alpha_{1i}-\Phi_{1i})},$$

then, the control objective of steering σ_{1i} and its derivative to zero can be achieved by selecting the control law as follows.

$$u_{1i} = -\int \alpha_{1i} sign(\sigma_{1i}) - \beta_{1i}\sqrt{|\sigma_{1i}|}sign(\sigma_{1i}), \tag{30}$$

The excitation control input then becomes:

$$E_{fi} = \frac{1}{I_{qi}}\left[u_{1i} + (x_{di} - x'_{di})I_{di}I_{qi} - T'_{doi}\frac{P_{ei}\dot{I}_{qi}}{I_{qi}}\right] \tag{31}$$

The control law (31) is valid for the whole practical operating region, except when $I_{qi} = 0$ which is not in the stability region of the closed-loop system. From (23) and the fact that $\dot{T}_i = 0$, η_i converges exponentially to 0 and the power angle δ_i, and the relative rotor speed ω_i also converges exponentially to δ_{iref} and 0, respectively. By virtue of relations (18) and (22), the generator terminal voltage V_{ti} and the active electric power P_{ei} converge to their reference value V_{tiref} and P_{mi} respectively.

3.2. High order sliding mode steam valve controller

Due to the physical constraint on the excitation voltage $(-3 < E_{fi} < 6)$ [1], a nonlinear control will be applied to the second input P_{ci} of the system to control the mechanical power input in order to further improve the transient stability of the power system described by (1)–(12).

From (4) it can be noticed that the turbine dynamic does not contain the steam valve control input explicitly. In the following analysis, we will use an auxiliary input to control the turbine output. To this end, we consider the mechanical power tracking error:

$$\widetilde{P}_{mi} = P_{mi} - P^*_{mi}, \tag{32}$$

and to ensure the exponential convergence of $\widetilde{P}_{mi}$ to zero, we take:

$$\dot{\widetilde{P}}_{mi} = -a_{2i}\widetilde{P}_{mi}, \quad \text{with} \quad a_{2i} > 0 \tag{33}$$

Next, we calculate the reference X^*_{ei} which is the unique solution of (33) as:

$$X^*_{ei} = \frac{1}{K_{mi}}[P_{mi} + T_{mi}\dot{P}^*_{mi} - T_{mi}a_{2i}(P_{mi} - P^*_{mi})]. \tag{34}$$

To obtain the control input P_{ci}, let us consider the following switching surface:

$$\sigma_{2i} = X_{ei} - X^*_{ei}, \tag{35}$$

whose second time derivative is:

$$\ddot{\sigma}_{2i} = \ddot{X}_{ei} - \ddot{X}^*_{ei}. \tag{36}$$

Substituting $\ddot{X}_{ei}$ obtained using (5) into (36), yields:

$$\ddot{\sigma}_{2i} = \frac{1}{T_{ei}}\dot{P}_{ci} - \frac{1}{T_{ei}}\dot{X}_{ei} - \frac{K_{ei}}{T_{ei}R_i\omega_s}\dot{\omega} - \ddot{X}^*_{ei} \tag{37}$$

which can be simplified into:

$$\ddot{\sigma}_{2i} = \frac{1}{T_{ei}}u_{2i} + G_{2i} \tag{38}$$

where $u_{2i} = \dot{P}_{ci}$ is an auxiliary control variable to be designed in order to satisfy the control objective of steering σ_{2i} and its derivative to zero and $G_{2i} = -\left(\frac{1}{T_{ei}}\dot{X}_{ei} - \frac{K_{ei}}{T_{ei}R_i\omega_s}\dot{\omega} - \ddot{X}^*_{ei}\right)$ is an uncertain term.

The super twisting algorithm is developed in this case using the same methodology as in Section 3.1. In order to satisfy Assumption (ii), the following inequality holds:

$$|G_{2i}| \leq \Phi_{2i} \quad \text{and} \quad 0 < K_{m2i} \leq \frac{1}{T'_{ei}} \leq K_{M2i}. \tag{39}$$

Under the above conditions, if the control gains are chosen as:

$$\alpha_{2i} > \frac{\Phi_{2i}}{K_{m2i}} \quad \text{and} \quad \beta_{1i}^2 \leq \frac{4\Phi_{2i}}{K_{m2i}^2}\frac{K_{M2i}(\alpha_{2i}+\Phi_{2i})}{K_{m2i}(\alpha_{2i}-\Phi_{2i})},$$

then, the control objective of steering σ_{2i} and its derivative to zero can be achieved by selecting the control law as follows.

$$u_{2i} = -\int \alpha_{2i} sign(\sigma_{2i}) - \beta_{2i}\sqrt{|\sigma_{2i}|}sign(\sigma_{2i}), \tag{40}$$

Remark 2. In the above controllers (31) and (40), it has been assumed that the mechanical power input P_{mi} is available. In addition, the control scheme is not implementable in practice because the time derivatives of I_{qi} cannot be obtained directly using numerical differentiation due to the presence of noise. Therefore, on-line adaptation law for P_{mi} and an estimation algorithm for $\dot{I}_{qi}$ are required to complete the design of the control scheme.

The complete block diagram of the proposed control scheme is shown in Fig. 1.

3.3. Nonlinear observer design

The unavailable time-derivative of I_{qi} required for the practical implementation of the control scheme can be estimated by using the real-time robust higher order sliding mode differentiator proposed in [22,27]. For the sake of notation, let

$$x_{i1} = I_{q_{is}} \quad \text{and} \quad \dot{x}_{i1} = x_{i2} = \dot{I}_{q_{is}}. \tag{41}$$

The current x_{i1} is considered as the sum of two terms

$$x_{i1} = x_{i10}(t) + \xi_i(t) \tag{42}$$

where $x_{i10}(t)$ is an unknown base signal assumed to be bounded and $\xi_i(t)$ is a bounded measurable noise with unknown features such that

$$|\xi_i(t)| \leq \epsilon_i \quad \text{and} \quad |\dot{\xi}_i(t)| \leq \nu_i, \quad |\ddot{\xi}_i(t)| \leq \varsigma_i. \tag{43}$$

$$|x_{i10}(t)| \leq C_{i0}, \quad |\dot{\xi}_{i10}(t)| \leq C_{i1}, \quad \text{and} \quad |\ddot{\xi}_{i10}(t)| \leq C_{i2}. \tag{44}$$

The form of the higher order sliding mode differentiator is given by:

$$\begin{aligned}
\dot{\hat{x}}_{i1} &= \hat{x}_{i2} - \hat{\lambda}_{i1}|s_{i1}|^{2/3}\text{sign}(s_{i1}) - k_{i1}\text{sign}(s_{i1}) \\
\dot{\hat{x}}_{i2} &= \hat{\lambda}_{i3}\hat{x}_{i3} - \hat{\lambda}_{i2}|s_{i2}|^{1/2}\text{sign}(s_{i2}) - k_{i2}\text{sign}(s_{i2}) \\
\dot{\hat{x}}_{i3} &= -\text{sign}(s_{i3})
\end{aligned} \tag{45}$$

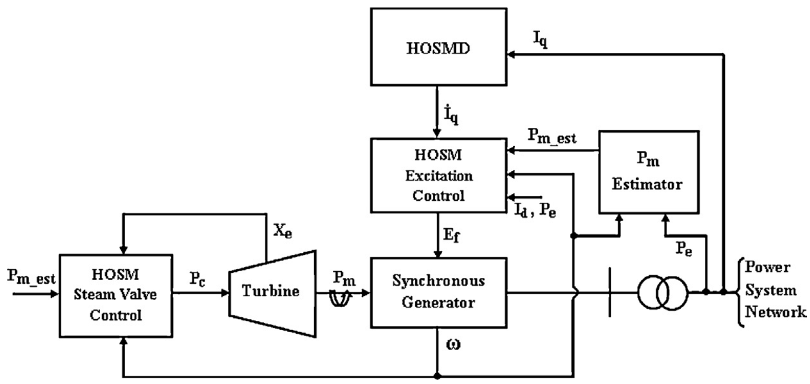

Fig. 1. Block diagram of proposed control scheme.

where $s_{i1} = \hat{x}_{i1} - x_{i1}, s_{i2} = \hat{x}_{i2} - \dot{\hat{x}}_{i1}$ are currents and time-derivative currents estimation errors, and $\hat{\lambda}_{ij}, j = 1, 2, 3$ are dynamic gains computed online using the following adaptive laws:

$$\begin{aligned}
&\dot{\hat{\lambda}}_{i1}(t) = |s_{i1}| \quad \text{for} \quad t < t_{fi1} \quad \text{and} \quad \hat{\lambda}_{i1}(t) = \hat{\lambda}_{i1}(t_{fi1}) \quad \text{for} \quad t \geq t_{fi1} \\
&\dot{\hat{\lambda}}_{i2}(t) = |s_{i2}| \quad \text{for} \quad t < t_{fi} \quad \text{and} \quad \hat{\lambda}_{i2}(t) = \hat{\lambda}_{i2}(t_{fi}) \\
&\text{for} \quad t \geq t_{fi} \quad \text{with} \quad t_{fi} = t_{fi1} + t_{fi2} \qquad (46) \\
&\dot{\hat{\lambda}}_{i3}(t) = s_{i2} \int_{\mathbb{R}} \text{sign}(s_{i2})dt \quad \text{for} \quad t < t_{fi} \quad \text{and} \\
&\hat{\lambda}_{i3}(t) = \hat{\lambda}_{i3}(t_{fi}) \quad \text{for} \quad t \geq t_{fi},
\end{aligned}$$

where t_{fi} is the finite time convergence of the differentiator (45). At time $t = 0$, $\hat{\lambda}_{i1}(0) = \hat{\lambda}_{i2}(0) = \hat{\lambda}_{i3}(0) = 0$.

The proof of the finite time convergence of the estimation errors s_{i1} and s_{i2} to zero can be found in [27].

Remark 3. The final proposed decentralized nonlinear adaptive control scheme is obtained by replacing the time-derivative of $I_{q_{is}}$ and the mechanical power input P_{m_i} with their estimates.

3.4. Global convergence and stability analysis

The global convergence and stability analysis taking into account the interconnections between the estimation algorithms for P_{mi}, $\dot{I}_{qi}$ and the nonlinear controllers (31) and (40) are based on the separation principle theorem [28]. The finite-time convergence of the observer/estimators allows us to design the observer/estimators and the nonlinear control laws separately, i.e., the separation principle is satisfied. The only requirement for its implementation is the boundedness of the states of the system in the operational domain.

4. Simulation results

The effectiveness and robustness of the proposed decentralized nonlinear coordinated excitation and steam valve control scheme has been verified by numerical simulations within the Matlab/Simulink environment software. The configuration of the multi-machine used is the Kundur 4-machine 2-area power system shown in Fig. 2. In order to compare and examine the interaction of the proposed scheme with other controllers, the 4 generators are first equipped with classical AVR/PSS controllers and steam valve PI regulators and then the classical AVR/PSS controllers and steam valve PI regulators of generators 1 and 3 are replaced with the proposed SOSM control scheme. The power system data are reported in Appendix A.2. To validate the proposed control scheme, we proposed four tests. The first is the test of robustness under extreme conditions with a 200ms symmetrical three phase

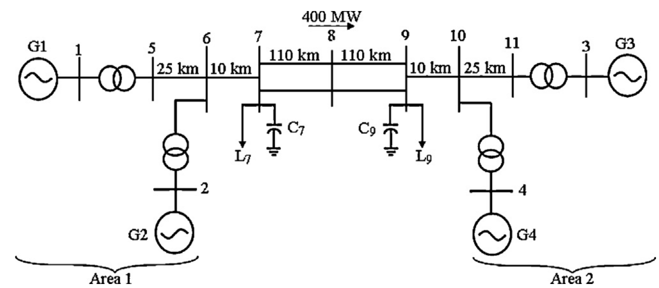

Fig. 2. Kundur 4-machine 2-area power system.

Table 1
Control scheme parameters.

Controller/observer	Parameter
Excitation controllers	$\beta_{0i} = 0.0001$; $a_{1i} = 2$
	$\beta_{1i} = 0.01$; $\alpha_{1i} = 2$
Steam valve controllers	$a_{2i} = 2$; $\beta_{2i} = 4$; $\alpha_{2i} = 15$
HOSMD	$k_{i1} = 2$; $k_{i2} = 5$
P_m estimator	$K_{i1} = 50$; $K_{i2} = 100$

short-circuit fault. The fault occurs at the end of one of the transmission lines between bus 7–8 (near bus 8). The fault has been conducted according to the following sequence:

1. At $t = 0$ s, the system is in pre-fault state.
2. At $t = 2$ s, a three phase short-circuit fault occurs in the transmission line.
3. At $t = 2.2$ s, the transmission line is restored and the system is in a post-fault state.

The second is a robustness test to the loss of measurable terminal voltage signal of all machines. Simulations were carried out following the sequence:

1. At $t = 5$ s, the system is in pre-fault state.
2. At $t = 6$ s, a 15% loss of measurable terminal voltage signal occurs on all machines.
3. At $t = 7$ s, the signal is restored and the system is in a post-fault state.

The third test is a 45% drop in mechanical power. The fault provides a large perturbation with a change in operating point. The fault has been conducted according to the following sequence:

1. At $t = 12$ s, the system is in pre-fault state.
2. At $t = 14$ s, a 45% drop in P_m occurs and the system operates under this condition in the post-fault state.

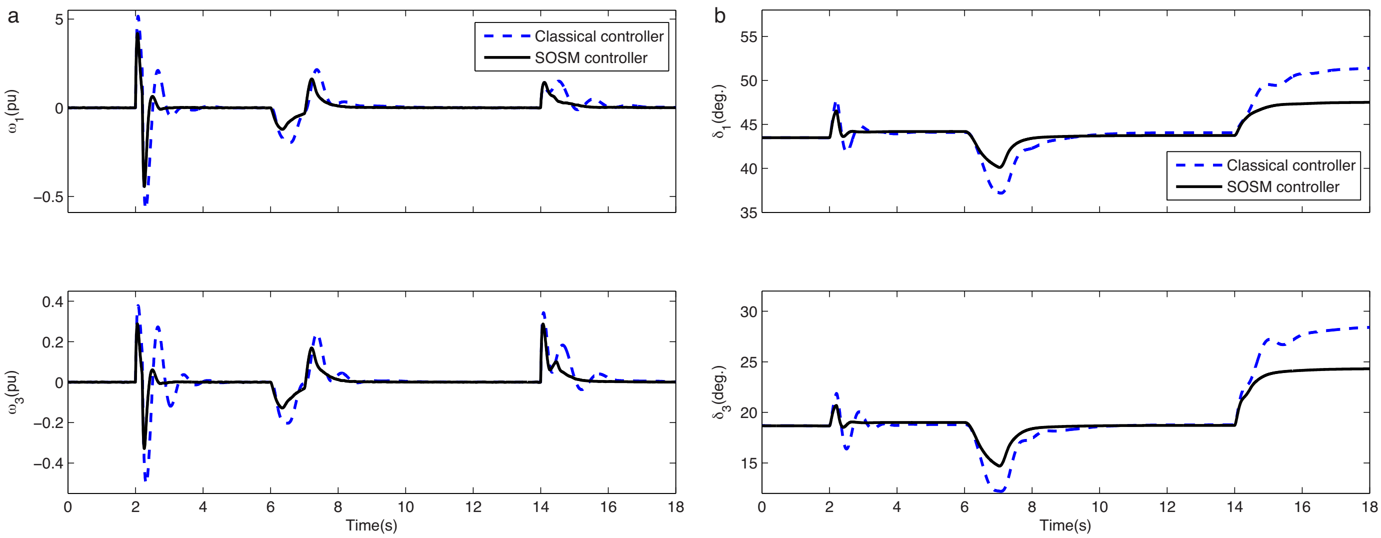

Fig. 3. Control response to 200 ms symmetrical three phase short-circuit fault, loss of measurable terminal voltage signal and variation of P_m (45% drop). (a) Relative rotor speed. (b) Power angle.

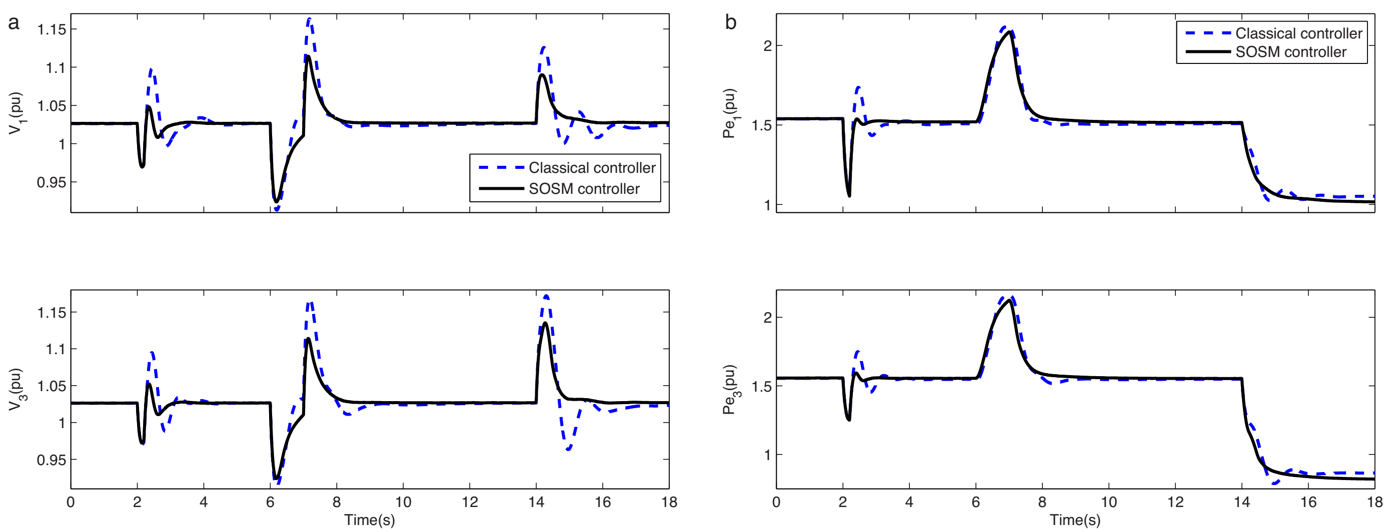

Fig. 4. Control response to 200 ms symmetrical three phase short-circuit fault, loss of measurable terminal voltage signal and variation of P_m (45% drop). (a) Terminal voltage. (b) Active electrical power.

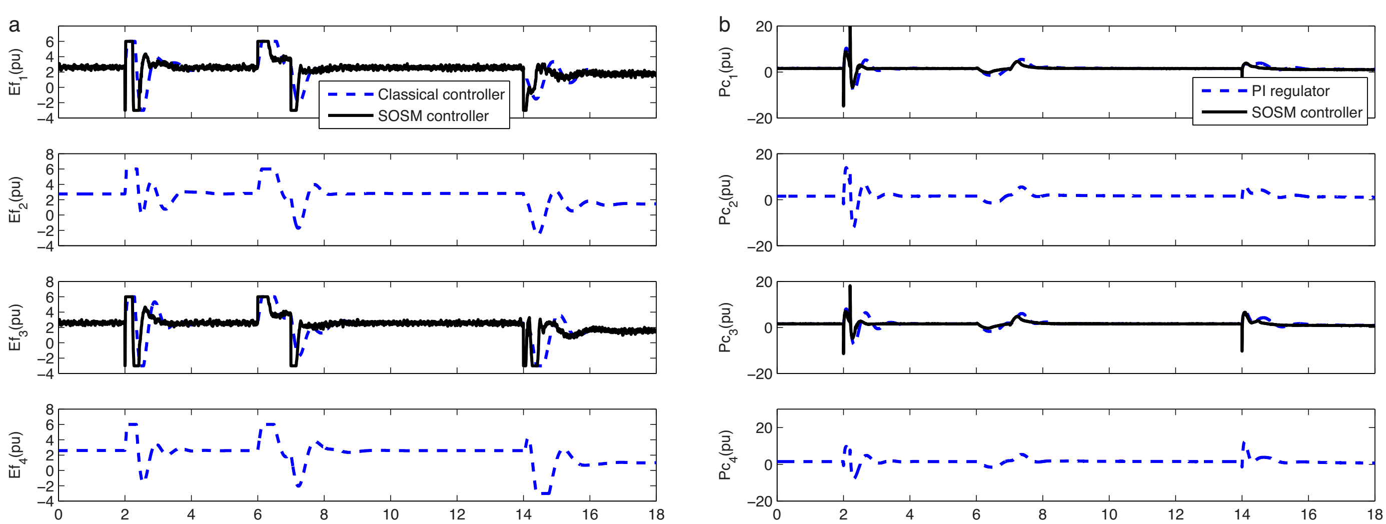

Fig. 5. Control response to 200 ms symmetrical three phase short-circuit fault, loss of measurable terminal voltage signal and variation of P_m (45% drop). (a) Excitation voltage. (b) Power control input.

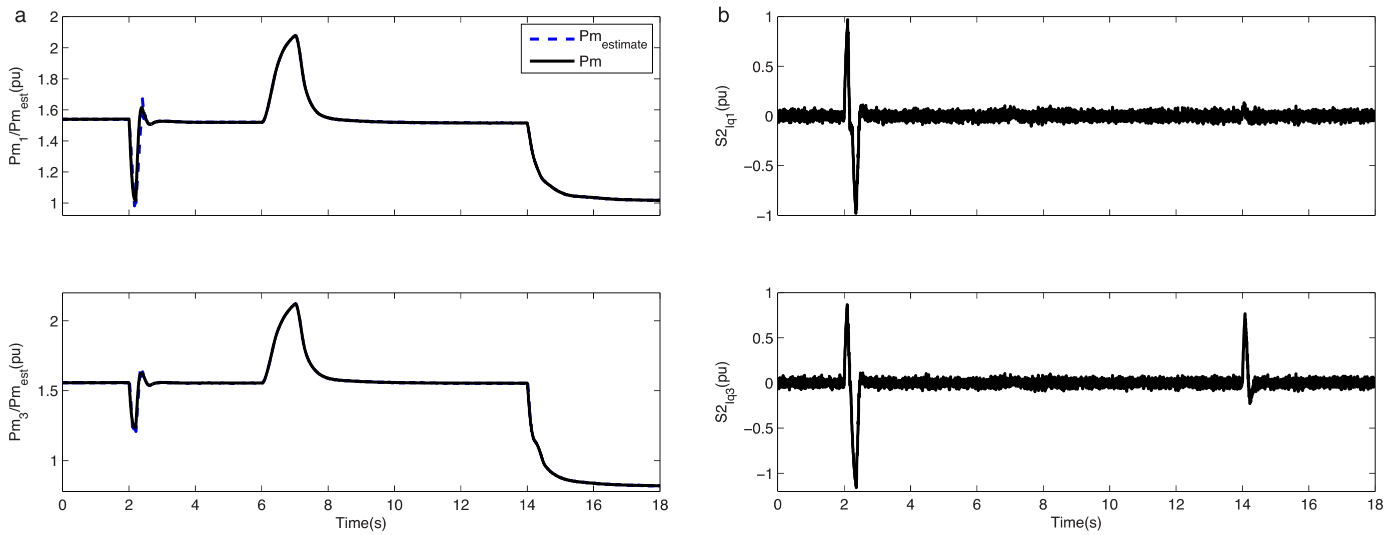

Fig. 6. Control response to 200 ms symmetrical three phase short-circuit fault, loss of measurable terminal voltage signal and variation of P_m (45% drop). (a) Mechanical power input and its estimate. (b) HOSMD estimation errors of the time derivative of I_q.

Due to space limitation, the first, second and third tests are merged on the same figures. All simulations have been conducted under noise conditions in the measured stator current. The magnitude of the noise reaches about 4% of the magnitude of the stator current. The tuning parameters used in the proposed controllers and observers/estimators are reported in Table 1. The classical AVR/PSS controller and steam valve PI regulator have been tuned using optimal control techniques.

4.1. Small signal stability analysis

From the simulation results, it can be observed that the relative rotor speeds, power angles, terminal voltages and active electric powers of generators 1 and 3 present more post-fault oscillations with the classical controller due to insufficient damping provided by the PSS. This damping is significantly improved with the proposed scheme. Thus the proposed scheme can also damp out some modes of small signal oscillations.

4.2. Large signal stability analysis

The comparative results for a 200 ms symmetrical three phase short-circuit fault are documented in Figs. 3–5 between 0 s and 4 s. It can be noticed from these figures that the proposed scheme quickly damps out oscillations and steers the system back to its steady state. Fig. 3 shows that with the proposed scheme, the relative rotor speeds and power angles present smaller over-shoots compared to the classical controller. In Fig. 4, it can also be seen that with the proposed scheme the terminal voltages and active electrical powers both settle to their pre-fault values very quickly with reduced overshoot and settling time. Therefore the proposed scheme effectively damps out oscillations and also significantly improves the transient stability and voltage regulation of the power system.

The comparative results for the lost of measurable terminal voltage signal of all machines are documented in Figs. 3–5 between 5 s and 12 s. The results clearly indicate that the proposed scheme is more robust and rapidly damps out oscillations.

The comparative results for a 45% drop in P_m are documented in Figs. 3–5 between 12 s and 18 s. One can also remark clearly from these figures that the proposed scheme quickly steer the system to its post-fault steady states. From Fig. 3, it can be noticed that with the proposed scheme, the relative rotor speeds and power angles are stabilized faster compared to the classical controller. Post-fault voltage regulation is also rapidly achieved.

From the simulation results, it can be seen that the proposed scheme rapidly and satisfactorily improve the transient stability, small signal stability, frequency stability and voltage regulation of the power system.

Table 2
Control response under parameter variation.

Parameter	Gen_1	Gen_2	Gen_3	Gen_4
H (s)	9.75 (+50%)	9.75 (+50%)	9.26 (+50%)	9.26 (+50%)
T'_{d0} (s)	12 (+50%)	12 (+50%)	12 (+50%)	12 (+50%)
$\Delta\delta$ (deg.)	0.89	2.5	1.02	2.529
$\Delta\omega$ (pu)	0.000502	0.0000212	0.000626	0.0000587

4.3. Control response to parameter variation

In practice, an accurate model of power system is not available and a fifth order model cannot represent the power generator unit precisely. For this reason, a fourth test has been carried out to investigate the robustness of the proposed control scheme with respect to system parameter variations or uncertainties. The fault has been carried out by changing the inertia constant H and the time constant T'_{do} of all machines, from their nominal values. The parameter variations introduced and the system response are shown in Table 2. From Table 2, it can be seen that generators equipped with the proposed scheme produced smaller deviations and can still provide consistent control performance even under parameter uncertainties. Hence it is not necessary to have an accurate model for designing the controllers.

Remark 4. The above comparative results show the effectiveness, robustness and superiority of the proposed scheme over the classical AVR/PSS controller and steam valve PI regulator. In addition, some important features can be underlined for the power system control scheme presented.

1 The proposed control scheme can be applied to any multimachine power system with n generators, m buses and k loads which can include other type of electrical elements such as FACTS, etc.

2 Each local controller requires only local information and the controller parameters are tuned in a decentralized way, i.e., the effect of other subsystems or controllers are considered as external perturbation.
3 The proposed control scheme can be easily implemented in real-time since some practical aspects have been taken into account such as:
- consideration of the physical constraint on the excitation voltage $(-3 < E_{fi} < 6)$;
- simulation under noise condition (Fig. 6);
- utilization of locally measurable information ($I_{di}, I_{qi}, P_{ei}, V_{ti}\ Q_{ei}$, ω_i and X_{ei});
- investigation of robustness with respect to parameter uncertainties;
- investigation of robustness with respect to loss of measurable signal;
- satisfactory interaction of the proposed controller with the classical AVR/PSS controller and steam valve PI regulator.

5. Conclusion

In this paper, a simplified decentralized nonlinear coordinated excitation and steam valve adaptive control scheme based on second order sliding mode technique using the supper twisting algorithm has been described. A modified high order sliding mode differentiator for the estimation of the time derivative of $I_{q_{is}}$ has also been presented. The simulation results show that the proposed nonlinear adaptive control scheme improves very satisfactorily the stability and performance of the power system under large disturbances (200 ms symmetrical three phase short-circuit fault), loss of measurable terminal voltage signal, change in operating point (45% drop in P_m) and parameter uncertainties. The comparative results have shown the effectiveness, robustness and superiority of the proposed scheme over the classical AVR/PSS controller and steam valve PI regulator.

Appendix A.

A.1. Power systems nomenclature

- δ_i Power angle of the ith generator in radians valid over the region defined by $0 < \delta_i < \pi$
- ω_s Synchronous machine speed in rad/s
- ω_i Relative rotor speed of the ith generator in rad/s
- H_i Inertia constant of the ith generator in s
- D_i Damping constant of the ith generator in pu
- E_{fi} Equivalent EMF in the excitation coil in pu
- K_{ci} Gain of excitation amplifier in pu
- u_{fi} Input to SCR amplifier in pu
- T'_{doi} Direct axis transient short-circuit time constant in s
- P_{ei} Active electrical power in pu
- Q_{ei} Reactive power in pu
- P_{mi} Mechanical power input in pu
- E_{qi} EMF in the quadrature axis in pu
- E'_{qi} Transient EMF in the quadrature axis in pu
- I_{fi} Excitation current in pu
- I_{di} Direct axis current in pu
- I_{qi} Quadrature axis current in pu
- x_{di} Direct axis reactance in pu
- x'_{di} Direct axis transient reactance in pu
- x_{adi} Mutual reactance between the excitation coil and the stator coil in pu
- V_{ti} Terminal voltage of the ith generator in pu
- X_{ei} Steam valve opening of the ith generator in pu
- P_{ci} Power control input of the ith generator in pu
- T_{mi} Time constant of the ith machine's turbine in s
- T_{ei} Time constant of speed governor in s
- K_{mi} Gain of the ith machine's turbine
- k_{ei} Gain of the ith machine's speed governor
- R_i Regulation constant of the ith machine in pu

Table 3
Generators nominal parameters.

Parameter	$\text{Gen}_{1,2}$	$\text{Gen}_{3,4}$
H (s)	6.5	6.175
X_d (pu)	1.8	1.8
x'_d (pu)	0.3	0.3
D (pu)	0.8	0.8
T'_{d0} (s)	8.0	8.0
ω_s (pu)	1	1
T_m (pu)	0.35	0.35
K_m (pu)	1.0	1.0
T_e (pu)	0.1	0.1
K_e (pu)	1.0	1.0
R (pu)	0.05	0.05

A.2. System nominal parameters

The generator parameters in per unit are taken from [25] and are given in Table 3.

References

[1] Y. Wang, G. Guo, D.J. Hill, Robust decentralized nonlinear controller design for multimachine power systems, Automatica 33 (1997) 1725–1733.
[2] G. Yi, J.H. David, W. Youyi, Nonlinear decentralized control of large power systems, Automatica 36 (2000) 1275–1289.
[3] X. Zairong, F. Gang, C. Daizhan, L. Qiang, Nonlinear decentralized saturated controller design for power system, IEEE Trans. Control Syst. Technol. 11 (2003 July) 539–547.
[4] G. Guoxiao, W. Youyi, J.H. David, Nonlinear output stabilization control for multimachine power systems, IEEE Trans. Circuits Syst. Part I 47 (2000 January) 46–53.
[5] G. Kenne, R. Goma, H. Nkwawo, F. Lamnabhi-Lagarrigue, A. Arzande, J. Vannier, An improved direct feedback linearization technique for transient stability enhancement and voltage regulation of power generators, Electr. Power Energy Syst. 32 (2010) 809–816.
[6] X. Zairong, L. James, Stabilization of generalized Hamiltonian systems with internally generated energy and application to power systems, Nonlinear Anal. Real World Appl. 9 (2008) 1202–1223.
[7] L.-M.J. de, K. Busawon, S. Acha-Daza, A robust observer-based controller for synchronous generators, Int. J. Control 23 (2001) 195–211.
[8] L.M. Fridman, Singularly perturbed analysis of chattering in relay control systems, IEEE Trans. Autom. Control 47 (2002 December 12) 2079–2084.
[9] B. Seddik, B. Djamal, B. Farés, Decentralized high order sliding mode control of multimachine power systems, Electr. Power Energy Syst. 43 (2012) 1081–1086.
[10] H. Huerta, A.G. Loukianov, J.M. Canedo, Robust multimachine power systems control via high order sliding modes, Electr. Power Syst. Res. 81 (2011) 1602–1609.
[11] M. Ouassaid, M. Maaroufi, M. Cherkaoui, Observer-based nonlinear control of power system using sliding mode control strategy, Electr. Power Syst. Res. 84 (2012) 135–143.
[12] A. Colbia-Vega, J. de León-Morales, L. Fridman, O. Salas-Pena, M.T. Mata-Jiménez, Robust excitation control design using sliding-modes technique for multimachine power systems, Electr. Power Syst. Res. 78 (2008) 1627–1634.
[13] V.I. Utkin, J. Guldner, J. Shi, Sliding Mode Control in Electromechanical Systems, Taylor and Francis, London, 1999.
[14] L. Fridman, A. Levant, Sliding Mode Control in Engineering. Higher Order Sliding Modes, Marcel Dekker, New York, 2002.
[15] M. Juan, F.V.A. Ramirez, E.C.G. Rosa, Transient stability improvement by nonlinear controller based on tracking, Electr. Power Energy Syst. 33 (2011) 315–321.
[16] G. Kenne, R. Goma, H. Nkwawo, F. Lamnabhi-Lagarrigue, A. Arzande, J. Vannier, Real-time transient stabilization and voltage regulation of power generators with unknown mechanical power input, Energy Convers. Manage. 51 (2010) 218–224.
[17] L. Qiang, S. Yuanzhang, M. Shengwei, Nonlinear Control System and Power System Dynamics, Kluwer Academic Publishers, 2001.
[18] M.J. Jin, W. Hu, F. Liu, S.W. Mei, Q. Lu, Nonlinear co-ordinated control of excitation and governor for hydraulic power plant, IEE Proc. Gener. Transm. Distrib. 152 (2005 July) 544–548.
[19] W. Youyi, J.H. David, Robust nonlinear coordinated control of power system, Automatica 32 (1996) 611–618.
[20] B. Wiktor, S. Jerzy, W. Tadeusz, Two-valve control of a large steam turbine, Control Eng. Pract. 10 (2002) 365–377.
[21] M. Bogdan, P. David, Three-level coordination in power system stabilization, Electr. Power Syst. Res. 111 (2014) 40–51.
[22] L. Sidhom, M. Smaoui, D. Thomasset, X. Brun, E. Bideaux, Adaptive higher order sliding modes for two dimensional derivative estimation, in: 18th IFAC World Congress Milano, Italy, August 28–September 2, 2011.
[23] Y. Yu, Electric Power System Dynamics, Academic Press, 1983.

[24] P.M. Anderson, A.A. Fouad, Power System Control and Stability, IEEE Press, NJ, 1994.
[25] P. Kundur, Power Systems Stability and Control, McGraw-Hill Inc., New York, 1994.
[26] G. Bartolini, G. Ferrara, A. Levant, E. Usai, On Second Order Sliding Mode Controllers. Variable Structure Systems, Sliding Mode and Non Linear Control, Lecture Notes in Control and Information Sciences, Springer-Verlag, London, 1999.
[27] G. Kenne, J.d.D. Nguimfack-Ndongmo, R.F. Kuate, H.B. Fotsin, Online simplified nonlinear controller for transient stabilization enhancement of DFIG in multimachine power systems, IEEE Trans. Autom. Control (2015), http://dx.doi.org/10.1109/TAC.2015.2427591.
[28] A. Levant, Higher-order sliding modes, differentiation and output-feedback control, Int. J. Control 76 (2003) 924–941.